

A Review on Autoignition in Laminar and Turbulent Nonpremixed Flames

Sanjeev Kumar Ghai and Santanu De

Abstract This chapter presents a condensed review on the autoignition in laminar and turbulent nonpremixed flames. Both experimental and numerical aspects are discussed. Fundamental studies on autoignition in turbulent flows revealed that random ignition spots are initially observed in the lean mixtures where the scalar dissipation rate is low. The mixture fraction corresponding to this lean mixture is usually referred as the “most reactive mixture fraction”. The increase in initial turbulent intensity and mixing delays autoignition. For most of the fuels, autoignition is observed as a two-stage process with a negative temperature coefficient. Besides, the physical and chemical properties of the fuels, the complex chemical kinetics also affect auto-ignition as well as combustion characteristics. Autoignition is also a dominant flame stabilization mechanism at the base of the lifted flames. Fundamental experimental investigations on autoignition in turbulent flows are very much limited, and most of the previous work is specifically focused on the Berkley vitiated coflow burner and the Cambridge burner. The combustion models developed so far can capture the trends observed in the experiments and the direct numerical simulation (DNS) studies. However, none of the combustion models developed so far can capture the trends quantitatively.

Keywords Autoignition • Turbulent combustion • Vitiated coflow • Lifted flame • PDF approach

List of abbreviations

DNS Direct numerical simulation
HCCI Homogeneous charge compression ignition
LPP Lean premixed pre-vaporized

S.K. Ghai (✉) • S. De
Department of Mechanical Engineering, Indian Institute of Technology Kanpur,
Kanpur 208016, UP, India
e-mail: snjv@iitk.ac.in

S. De
e-mail: sde@iitk.ac.in

DME	Dimethyl ether
CI	Compression ignition
PM	Particulate matter
RCM	Rapid compression machine
NTC	Negative temperature coefficient
MILD	Moderate and intense low oxygen dilution
RANS	Reynolds averaged Navier Stokes simulation
LES	Large eddy simulation
CMC	Conditional moment closure
PDF	Probability density function
IEM	Interaction by exchange with the mean
EMST	Euclidean minimum spanning tree
HRR	Heat release rate

Nomenclature

Y_I	Mass fraction of species I
N	Scalar dissipation
Z	Mixture fraction
η	Sample space of mixture fraction
ξ	Conditional variable
$Q(\eta, \mathbf{x}, t)$	Conditional expectation
$\dot{\omega}$	Reaction rate
$\tilde{P}(\xi, \chi, \mathbf{x}, t)$	Joint scalar PDF

1 Introduction

The autoignition or self-ignition of a flammable mixture is a fundamental problem in combustion, where we deal with the transition from a slowly reacting state to a fully burning state corresponding to combustion at high temperature. A simple experiment on autoignition may be carried out where the initial temperature of a uniform stagnant fuel-air mixture in a close vessel is slowly raised until the mixture ignites at a temperature, which may be referred as the autoignition temperature. The time taken by the mixture to ignite is referred as the autoignition time or ignition delay time. Due to the increasing rate of chemical reactions with increasing temperature, even the very weak reaction starts to generate sufficient heat, which causes a further rise in temperature and thereby resulting in a faster heat release rate. Thermal runaway eventually takes place at an autoignition time that depends on the initial temperature, the concentrations of reactants, the nature of the fuel, and the

pressure. The autoignition temperature of a fuel-air mixture provides useful information on how various compounds autoignite, but it does not provide any fundamental insights on the autoignition process and how it affects the flow behaviour in general.

Autoignition of turbulent fuel jets issued into a stagnant or coflowing oxidizer stream, and the subsequent flame stabilization is a well-known problem frequently encountered in Diesel engines, ramjets, and gas turbine combustors. The effect of turbulence on autoignition is not only a fundamental topic of research, but it is also crucial for the development of the next generation combustion systems for transportation and power generation such as homogeneous charge compression ignition (HCCI) engines and lean premixed pre-vaporized (LPP) gas turbines. Development of these industrial combustion systems is hindered by our capabilities to predict the interaction between turbulence and the slow chemistry leading to autoignition. It is needless to say that a better understanding and capability to predict the autoignition will facilitate the development of energy-efficient and environment-friendly combustors. In the practical combustors, the presence of considerable fluctuations of velocity, temperature, and mixture composition greatly impacts autoignition and the subsequent flame development process. With the ever-increasing requirement of emission regulation, alternative fuels or fuel additives are routinely being used and tested in Diesel engines and land-based gas turbines. The physical and chemical properties of the new fuels and their complex chemical kinetics are likely to affect their atomization, evaporation, mixing, auto-ignition, as well as combustion characteristics. A thorough understanding of the physical processes and their complex interactions are not available. Besides experimental capabilities, numerical models for these complex physical phenomena need to be developed in order to speed up the design, development, and optimization of the combustion chambers of these practical systems.

With the advancement of combustion diagnostics and numerical tools and the availability of more precise information on the chemical kinetics, auto-ignition of gaseous- and liquid fuels need to be revisited to address some of the fundamental aspects such as the development of ignition kernel, flame propagation and flame stability in the inhomogeneous mixtures. In the last decade, two different burners were developed to investigate auto-ignition in the inhomogeneous mixture, namely, vitiated co-flow burner [1] and preheated coflowing air burner [2, 3]. Besides revealing the vital information on autoignition under inhomogeneous mixture conditions, the experimental data from these burners have been routinely used for development of turbulent combustion models. A comprehensive database is now available [1–5] on autoigniting turbulent jet flames for different fuels. The prevailing auto-ignition mechanism is found to be consistent with those revealed by the direct numerical simulation (DNS) studies. In these burners, reaction kernels develop at some distance downstream of the fuel injector. These ignition kernels eventually initiate the flame development.

The book chapter amalgamates the knowledge on autoignition under laminar and turbulent conditions. In the subsequent sections, a review will be presented on fuel properties and its effects on autoignition, various experimental configurations employed to study autoignition under laminar and turbulent conditions, and modelling approaches for turbulent combustion. Towards the end of this chapter, major conclusions are drawn, and future recommendations are presented.

2 Fuel Properties

The properties of the fuel play an important role due to its applicability in different operating conditions. Due to the stringent emission regulations, combustion community is widely interested in replacing the conventional fuels with the alternative fuels. The fuel replacement in the internal combustion engines and gas turbine combustors also affects the combustion and emission characteristics. The physical and chemical properties of various fuels, e.g., dimethyl ether (DME), Diesel, butane, propane, hydrogen, and gasoline are shown in Table 1 [6–8]. In compression-ignition (CI) engines, ignition occurs due to self-ignition of the fuel. Autoignition temperature is one of the very important properties of the fuel in CI engines. The modern combustors are also being developed for alcohols, biofuels, synthetic and renewable fuels and different fuel mixtures.

Table 1 Physical and chemical properties of different fuels [6–8]

Property	DME	Diesel	Butane	Gasoline	Propane	Hydrogen
Chemical formula	CH_3OCH_3	C_8 to C_{25}	C_4H_{10}	C_7H_{16}	C_3H_8	H_2
Molecular weight	46.07	96~	58.13	100.2	44.11	2.02
Vapour pressure at 20 °C (bar)	5.1	<0.01	8.4	–	2.1	–
Boiling temperature (°C)	–25	≈150–380	–0.5	38–204	–42.1	–253
Liquid density at 20 °C (kg/m^3)	660	800–840	610	719.7	501	70.8
Liquid viscosity at 25 °C (kg/ms)	0.12–0.15	2–4	0.2	–	0.2	–
Gas specific gravity (vs air)	1.59	–	2.01	–	1.52	–
Lower heating value (MJ/kg)	28.43	42.5	45.74	44.5	46.36	119.93
Cetane number	55–60	40–55	–	80–100	5	130
Stoichiometric A/F ratio (kg/kg)	9.0	14.6	14.8	14.5	15.7	34.3
Enthalpy of vaporization at NTP ^a (kJ/kg)	460(–20 °C)	250	390	–	426	448.69
Auto-ignition temperature (K)	508	523	638	501–744	743	858
Lower explosion limit (vol.%)	3.0–3.4	0.6	1.9	1.0	2.1	4.0
Upper explosion limit (vol.%)	17–18.6	6.5–7.5	8.4	7.6	9.4	75
Minimum ignition energy (mJ)	0.29	–	0.305	0.24	0.26	0.02

The physical and chemical properties of these new fuels determine whether they are suitable for different industrial applications. As an example, DME is a promising alternative fuel in Diesel engines and is being considered as a possible substitute for natural gas in power-generation applications. It is a clean-burning, non-toxic fuel with low soot formation potentials and PM emissions, which can be synthesized from natural gas, coal, and renewable fuels such as biomass and ethanol. DME exhibits Diesel-like performance due to its high Cetane number (55–60) [8] at the same time it offers propane-like handling properties due to its low boiling point (-25°C) at atmospheric conditions. It has a lower autoignition temperature than Diesel, and it has a higher flammability range compared to other hydrocarbons due to the presence of the large oxygen content. However, it has a lower heating value compared to Diesel. Therefore, to produce the same output, we need to supply more DME in the combustion chamber. Also, very little is known about the fundamental combustion processes of DME-fuelled systems under highly turbulent conditions and at different operating pressures. Hence, fundamental understanding of the complex interplay between chemistry and turbulence is essential for speedy implementation of DME as an alternative fuel for internal combustion engines and gas turbines.

3 Experimental Approaches

In this section, fundamental findings and experimental approaches for autoignition in laminar and turbulent non-premixed flows are discussed. Experimental facilities to study autoignition are very limited till date. Most of the experiments are usually conducted under the ambient pressure conditions [1, 2]. Practical systems are very complex for experimental investigations. Replication of these complex systems in a laboratory is not only difficult and expensive, but rather a kind of impossible task. To gain fundamental insights on autoignition, simple lab scale setups have been designed and developed with optical access and good illumination. These experimental setups are designed with well-defined inlet boundary conditions to facilitate numerical model development. The various burner configurations presented in this section (e.g., lifted jet flames in the vitiated coflow, MILD combustion in the jet in hot coflow configuration, confined turbulent hot coflow burner and counterflow flame setup) demonstrate aspects of autoignition.

High spatial and temporal resolutions are also needed to study the transient phenomenon of turbulence-flame interactions. With the state-of-the-art combustion diagnostics systems, simultaneous measurements of the flow- and scalar fields are now possible to achieve complete physical insights of the problem. Various experimental techniques such as laser Doppler velocimetry (LDV), particle imaging velocimetry (PIV), phase Doppler anemometry (PDA) are used for flow field measurements and Mie scattering, laser absorption spectroscopy (LAS), planar laser-induced fluorescence (PLIF), 1D Raman/Rayleigh scattering, coherent

anti-Stokes Raman spectroscopy (CARS) are used for scalar field measurements. Until early 1990's, experiments on autoignition had been limited to shock tubes, flow reactors and rapid compression machine (RCM). While each of these devices has own merits, but their application is restricted to certain specific conditions. As an example, flow reactors have limitations of maximum achievable pressure and temperature limits, while shock tubes are limited by short ignition time. On the other side, RCM is suitable for high-temperature and pressure applications with comparatively higher ignition time compared to the shock tubes.

3.1 Autoignition in Rapid Compression Machine

A schematic for the RCM is shown in Fig. 1. RCM operates at a compression ratio of 10:1. Primarily it is used to investigate chemical kinetics [9]. Carlier et al. [9] conducted consecutive experiments on autoignition of butane both at low and high pressures in RCM. They have observed autoignition as a two-stage process at low temperature, and their results indicate the appearance of negative temperature coefficient (NTC) by the autoignition delay times at high pressure. Also, they compared the measurements with the numerical predictions using available reaction mechanisms [11] by adjusting the rate constants (shown in Fig. 2). Improvement in the available reaction mechanisms was suggested in order to capture autoignition within the broad temperature and pressure range of extremely varying experimental conditions. Minetti et al. [12] investigated the oxidation and autoignition of the

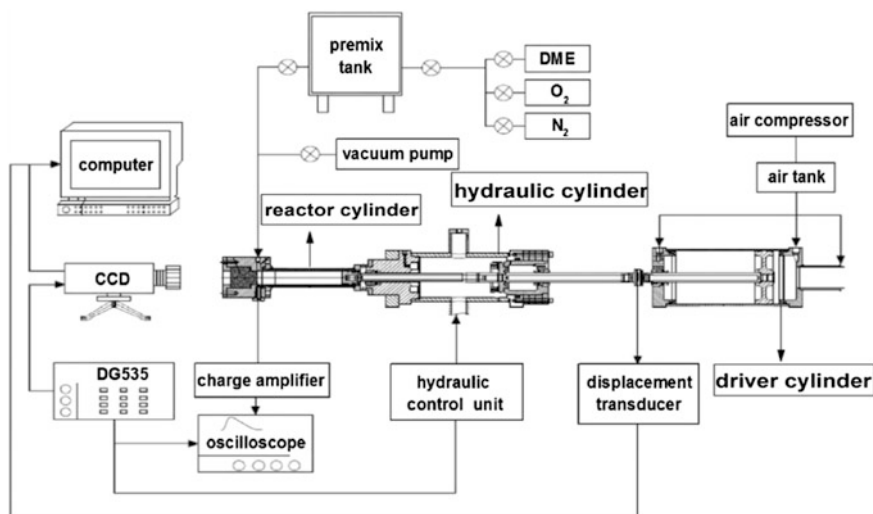
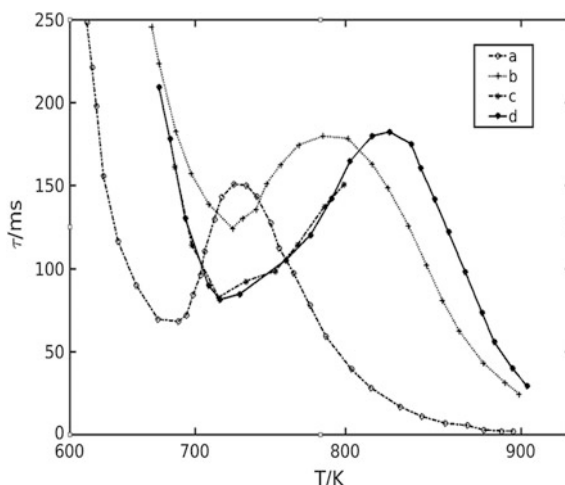


Fig. 1 A schematic of rapid compression machine [10]

Fig. 2 Ignition delay in RCM [9] for a butane oxygen-inert mixture: **a** experimental predictions, butane-oxygen (1 N₂, 1 Ar), **b** butane-oxygen-Ar, **c** numerical results using the mechanism of [11], and **d** numerical results using a revised version of [11]

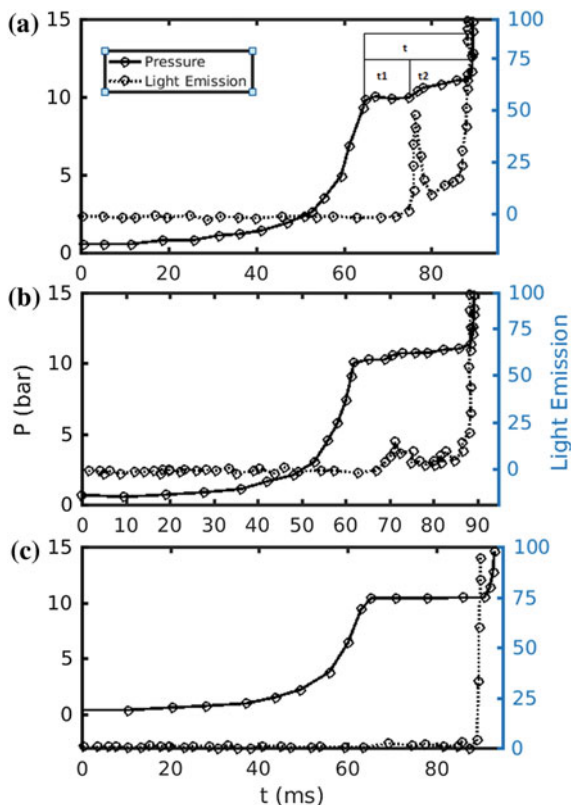


butane-air mixture in RCM at 700–900 K temperature and 9–11 bar pressure. A transition from the two-stage to a single-stage autoignition was observed under certain experimental conditions. Figure 3a shows two-stage autoignition within a temperature range of 700–760 K. In the first stage, an initial delay of t_1 was recorded, followed by an increase in pressure along with the significant emission of light in the second stage with a delay time t_2 . However, for temperatures above 850 K, ignition occurred in single-stage only (Fig. 3c) with a decrease in the total delay time. In a recent study [13], the autoignition of tetralin/O₂/N₂ mixture in RCM failed to produce any evidence of NTC behaviour.

3.2 Autoignition in Flow Reactor

Flow reactors work based on the principle of direct mixing between fuels and flowing stream of hot oxidizer. The combustible mixture ignites over a long distance from the point of injection. Flow reactors have long ignition delay and particularly suitable for constant pressure applications. Also, the application is somewhat restricted to low-temperature $T < 1200$ K and intermediate pressure range of 1–20 bar. The flow reactors offer the advantage of having relatively simple measuring techniques due to the large spread of the reaction zone. Plenty of literature is available on the experimental investigations of autoignition using flow reactors [14–18]. Pressurized flow reactor was used to study autoignition of hydrogen in air using OH chemiluminescence technique [15]. The results revealed that the surface reaction has a serious impact on autoignition delay.

Fig. 3 Diagram showing pressure and light emission during the compression and autoignition for different stoichiometric ratio. Core temperature: **a** $T_c = 749$ K, **b** $T_c = 796$ K, **c** $T_c = 818$ K [12]



3.3 Autoignition in Shock Tube

As the name suggests, shock tube uses the shock wave compression for bringing the reactants to a reactive state. Shock tubes are ideal for determining shorter ignition delay of the order of few milliseconds at high temperature. Autoignition of iso-cetane was investigated in a shock tube [19] and a new reaction mechanism was developed without changing the rate constants. The results with the newly developed reaction mechanism are found to be in reasonably good agreement with the experimental measurements. Autoignition of methyl decanoate [20], demonstrated the NTC behaviour for ignition delay at high pressure, which is comparable to that of *n*-decane. However, at low pressure, ignition delay time was found to be shorter than that of *n*-decane. Also, methyl decanoate demonstrates different oxidation mechanisms at low- and high temperatures. With the decrease in temperature, reactivity of methyl decanoate also reduces similar to that of *n*-decane.

3.4 Autoignition in Laminar Non-premixed Flows

The counterflow- or opposed-jet flow burner setup is the most widely used configuration for investigation of autoignition in laminar non-premixed flames (Fig. 4). Several experiments on autoignition have been performed in the counterflow configuration for a wide variety of fuels and at different operating conditions (such as temperature, pressure, and dilution). The results demonstrate the existence of a critical strain rate for autoignition. Autoignition is favoured for laminar non-premixed flames with low scalar dissipation rate. The same trend had also been observed in numerical simulations [22]. Autoignition of the H_2/N_2 mixture in an opposed flame configuration was examined with heated air stream as the oxidizer within a pressure range 0.1–6.0 atm [23]. It was found that under all ambient pressure conditions, the ignition temperature monotonically increases with an increase in the flow strain rates. However, under atmospheric pressure condition, the ignition temperature was found to be insensitive to changes in the flow strain rate. This is clearly shown in Fig. 5.

When hydrogen was added in methane, two-stage ignition took place, where the first stage is dominated by radical runaway followed by a thermal feedback mechanism in the second stage [24]. The two-stage ignition improves the ignition of methane significantly. The effect of N_2 dilution on ignition temperature was also investigated for DME jets in a counter-flow flame configuration with heated air as the oxidizer [25]. At constant pressure, nitrogen dilution in DME decreases the ignition temperature. Further, the ignition temperature also decreases with an increase in pressure. The results were found to be consistent with the previous experimental observations reported in previous literature [23, 24]. The flame structure of laminar CH_4/N_2 jet under moderate and intense low-oxygen-dilution (MILD) conditions in hot coflow was examined by Sepman et al. [26]. The flame height decreased with hydrogen addition. However, the maximum flame temperature and the thickness of combustion zone remained almost unaffected by the

Fig. 4 A schematic for counter-flow diffusion flame [21]

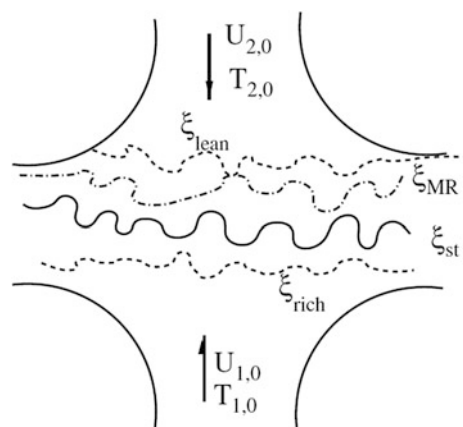
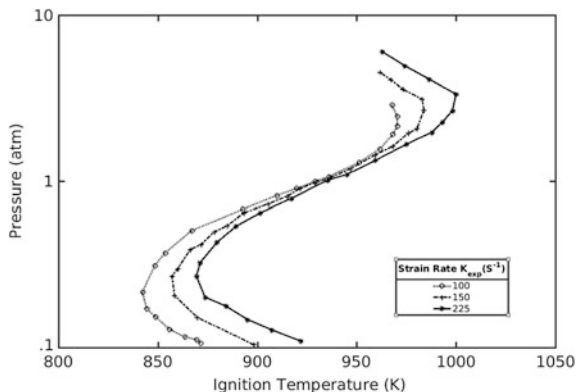


Fig. 5 Ignition temperatures versus pressure at different strain rate [23]



addition of hydrogen. The flame structure and NO formation at different preheat conditions were also investigated [27]. Under the MILD conditions, NO formation decreases considerably.

3.5 Autoignition in Turbulent Non-premixed Flows

Autoignition in turbulent nonpremixed flows is important from both industrial and academic perspective. The industrial burners are complex in nature due to their complex geometry and flow features. In order to gain physical insights of autoignition in inhomogeneous mixtures, simple experimental burner configurations have been developed in the past couple of decades. The Berkley burner was developed [1] to understand the physics behind the stabilization of lifted flames. They replicated a complicated process of exhaust gas recirculation with a very simple laboratory-based experimental setup in which the central jet is stabilized by hot products of lean H_2 /air combustion. The schematic for the same is shown in Fig. 6. Their results concluded autoignition along with flame propagation as the relevant stabilization mechanism for lifted flames. However, they recommended further studies to confirm this phenomenon. The open flow configuration of the Berkley burner [1] provides a good optical access, which facilitates point and planar diagnostics for visualization of pre-ignition regions, autoignition spots, and the ensuing flamelets.

Mastorakos and co-workers [2, 3] experimentally investigated auto-ignition of diluted H_2 and prevaporized n -heptane jets in a confined turbulent hot co-flow (CTHC) burner. The schematic for the same is shown in Fig. 7. This burner has optical access and is well-suited for autoignition experiments under turbulent conditions. The experimental database from this burner has been used for development of turbulent combustion models.

Fig. 6 Schematic of Berkley vitiated coflow burner [28]

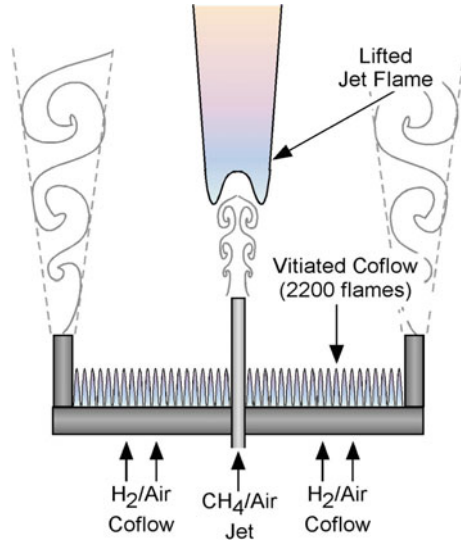
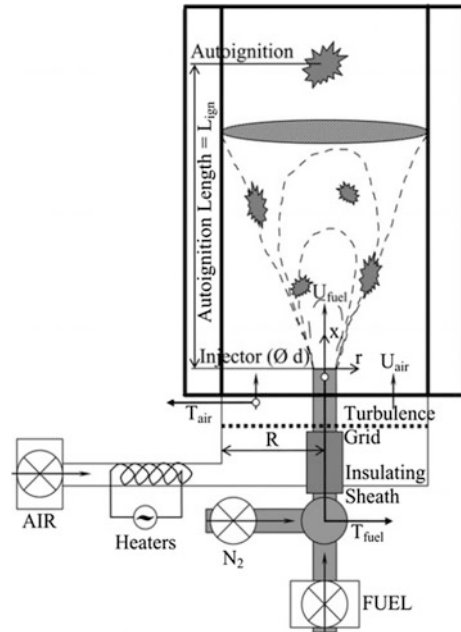


Fig. 7 Schematic burner configuration used by Markides and Mastorakos [2]



During the experiments, auto-ignition kernels were identified using optical techniques, and their axial locations were measured by OH- radical chemiluminescence images. The auto-ignition length (and hence ignition delay time) increases with a decrease in the co-flow temperature (as shown in Fig. 8) and with an increase

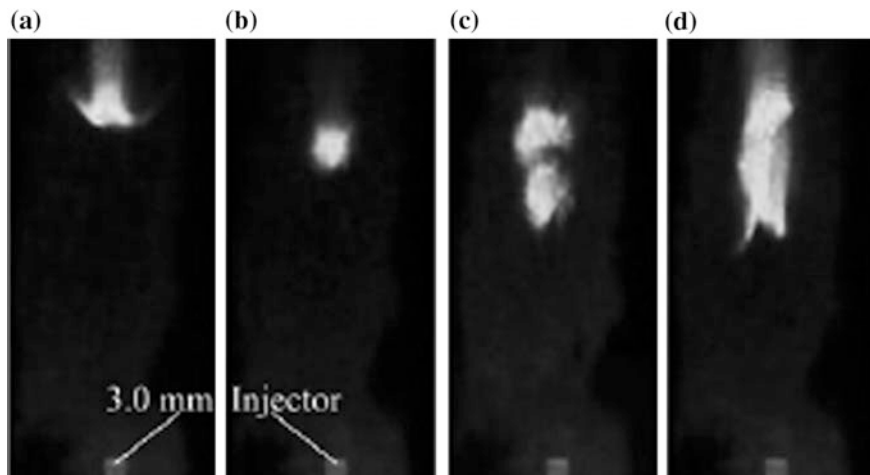


Fig. 8 Instantaneous raw OH chemiluminescence snaps for the autoigniting H_2 jet: **a–c** for $T_{\text{air}} = 1000$ K, whereas **d** for $T_{\text{air}} = 1020$ K [2]

in the jet and co-flow velocity. Also, the results showed that the turbulent mixing delays auto-ignition. Four different regimes, namely “no ignition”, “random spots”, “flashback” and “lifted flame” were observed under different operating conditions. The optical imaging technique used by Mastorakos and co-workers [2, 3] was later used to explore turbulent mixing and auto-ignition of acetylene jets in inhomogeneous mixtures [29]. A parametric study was conducted wherein the effects of turbulent intensity, turbulent length scale, and injector diameter are considered. By retaining a constant level of turbulent intensity, an increase in the injector diameter resulted in an increase in the auto-ignition length. However, a simultaneous increase in the length scale and a decrease in the turbulent intensity shortened the auto-ignition length. Further, the frequency of appearance of auto-ignition increases with an increase in the air velocity.

Roubaud et al. [30] investigated autoignition and oxidation mechanisms of alkylbenzenes in the range of 600–900 K at pressure above 14 bars. Their results showed the double peroxidation and low-temperature branching phenomena during isomerization step when benzylic radicals combine with an oxygen molecule. Using a burner similar to the one used by Cabra [1] and high-speed Schlieren video imaging technique, Johannessen et al. [31] investigated unsteady H_2/N_2 flames in a vitiated co-flow. It was seen that nitrogen dilution increases the frequency of ignition up to a certain maximum value, beyond which the frequency of ignition decreases. The experimental results also established that re-ignition is primarily controlled by chemical kinetics and turbulent mixing. Also, the high-speed planar images obtained using Rayleigh scattering technique for a pulsed turbulent jet flame in a vitiated coflow [32] established that auto-ignition is most likely to occur at the periphery of the fuel jet, where the mixture is very lean and scalar dissipation rate is

low. By using high-speed shadowgraphy, a two-stage ignition was reported during the transient injection of DME under high-pressure conditions [33] for reported operating conditions. Oldenhof et al. [34] experimentally investigated the ignition of impulsively started jets of natural gas in heated co-flow using particle image velocimetry (PIV) and Planar Laser Induced Fluorescence (PLIF) techniques. The jet leaving the nozzle was laminar initially, which suddenly transitioned to a turbulent jet. During the laminar phase, combustion was not observed and large ignition delay time was reported during the process of transition to turbulent phase. It is believed that the presence of the large-scale inhomogeneities increases the ignition delay time.

Chen and co-workers [35] performed an experimental study on the combustion characteristics in an HCCI engine by diluting the natural gas with DME. Their investigations predicted that when DME was mixed with the natural gas in small proportions, the engine can run over a comparatively large load range with higher thermal efficiency compared to the Diesel engine and also reduces the ignition delay and NO_x emissions. Venkatesan et al. [36] conducted experiments using DME as an ignition improver in a hydrous methanol-fuelled HCCI engine. The combustion characteristics of methanol and ethanol were also investigated under HCCI mode of operation [37]. It was found that methanol auto-ignites faster than ethanol in HCCI conditions.

4 Turbulent Combustion Models

In the Reynolds-Averaged-Navier-Stokes (RANS) and large eddy simulations (LES) approach, the transport equations for the temperature and species mass fractions contain mean/filtered chemical source terms. Since the chemical source term is a nonlinear function of species mass fractions and temperature, accurate evaluation of the mean chemical source term becomes difficult. The so-called ‘direct closure’ approach is known to introduce erroneous values of the mean/filtered chemical source terms. This ‘closure of mean/filtered chemical term’ has been the central difficulty in RANS/LES of reacting flows.

Turbulent combustion may be modelled either assuming it is controlled by turbulent mixing (e.g., eddy breakup (EBU), and eddy dissipation models (EDM), etc.) or via statistical approaches, where the statistical properties of intermediate states are described using a PDF [38]. With the joint composition PDF, $\tilde{P}(\rho, Y_1, \dots, Y_N, T; x, t)$, the mean burning rate may be estimated as

$$\dot{\omega}_{Y_i}(x, t) = \int_{\rho, Y_1, \dots, Y_N, T} \dot{\omega}_{Y_i}(\rho, Y_1, \dots, Y_N, T) \tilde{P}(\rho, Y_1, \dots, Y_N, T; x, t) d\rho dY_1, \dots, dY_N dT \quad (1)$$

The PDF may be determined either by presumed PDF method [39] or transported PDF method [38]. In the presumed PDF method, an empirical expression for the PDF is chosen. Since the shape of the PDF usually depends on the local physical conditions, a few parameters of the PDF are computed at each physical location based on the balance equations of the first several moments, usually the mean and variance. The presumed PDF method is often used to model one variable. It becomes difficult to model more than one variable with a presumed joint PDF. For such problem, assumption is made that the variables are statistically independent and model the single variable with presumed PDF:

$$\tilde{P}(\psi_1, \psi_2, \dots, \psi_N) \approx \tilde{P}_1(\psi_1) \tilde{P}_2(\psi_2) \dots \tilde{P}_N(\psi_N) \quad (2)$$

Alternatively, significant efforts have been taken to simplify the expression of the joint PDF, $\tilde{P}(\rho, Y_1, \dots, Y_N, T; x, t)$. For instance, the composition space Y_1, \dots, Y_N is replaced with a conserved scalar; the joint PDF is presumed to have an empirical expression. Another class of combustion models assumes that the chemical reaction occurs in thin layers separating fuel and oxidizer (high Damköhler number $Da \gg 1$ limit). The reaction zone is viewed as a collection of laminar flamelets. Coherent flamelet and flame surface density models are introduced for premixed turbulent combustion [40]. For non-premixed flames, hypotheses are formulated to construct different models such as (1) infinitely fast chemistry (IFC) model, (2) flamelet models and (3) conditional moment closure (CMC) method. First two models are applicable in the limit of $Da \gg 1$. For non-premixed combustion, the joint PDF $\tilde{P}(\rho, Y_1, \dots, Y_N, T; x, t)$ is greatly simplified using a chemistry-independent conserved scalar, namely mixture fraction ξ .

4.1 Laminar Flamelet Model

The flamelet assumption takes into account the non-equilibrium effects. This model has been developed both for non-premixed [39] as well as premixed [41] combustion. It is derived based on the assumption that the thickness of the reaction zone is sufficiently small compared to the Kolmogorov length scale, and molecular diffusion can determine its internal structure without the influence of turbulence. The flamelet model views the turbulent diffusion flame as an ensemble of thin, laminar, locally one-dimensional structures called flamelets embedded within the turbulent flow field. The ensemble is weighted by a presumed PDF to produce the turbulent ‘flame brush’. Instead of calculating the reaction rate, the composition space is determined from a pre-calculated laminar flamelet library. The coupling between non-equilibrium chemistry and turbulence is achieved by the statistical description of two parameters: the mixture fraction ξ and the scalar dissipation rate χ . The mean value of any scalar Ψ (temperature and compositions) is calculated by

$$\tilde{\psi}(x, t) = \int_0^1 \int_0^\infty \psi(\xi, \chi) \tilde{P}(\xi, \chi; x, t) d\chi d\xi \quad (3)$$

Here $\tilde{P}(\xi, \chi; x, t)$ is the joint PDF of the mixture fraction and the scalar dissipation rate, and these two parameters are assumed to be statistically independent

$$\tilde{P}(\xi, \chi; x, t) = \tilde{P}_\xi(\xi; x, t) \tilde{P}_\chi(\chi; x, t) \quad (4)$$

The steady flamelet equation can be given as

$$\rho \frac{N_{st}}{2} \frac{\partial^2 Y_K}{\partial Z^2} + \dot{\omega}_K = 0 \quad (5)$$

where, N_{st} is the scalar dissipation at the stoichiometric value.

4.2 Transported PDF Model

In the transported PDF method, the turbulent flow is described by the transport equation of joint PDF of the velocity and scalars in the flow field namely mass fractions of species and enthalpy. This equation can be derived from Navier-Stokes equations and conservation equation for scalars [38]. In this formulation, the nonlinear chemical source term does not require any closure. However, terms involving molecular mixing in reactive scalar space, fluctuating pressure term and PDF transport in velocity space by viscous stresses require closure models. The qualitative performance of the PDF method largely depends on the accuracy of submodels used to close these terms [42]. None of the molecular mixing models namely, interaction by exchange with the mean (IEM), linear mean-square estimation (LMSE), mapping closure (MC) and Euclidean minimum spanning tree (EMST) [43] includes a physically realistic representation of scalar dissipation rate to capture phenomenon such as local extinction, re-ignition [44]. Theoretically, the transported PDF method can treat the arbitrary complex chemistry without any assumption. The transport equation of joint scalar PDF may be written as

$$\begin{aligned} \frac{\partial}{\partial t}(\rho P) + \frac{\partial}{\partial x_i}(\rho u_i P) + \frac{\partial}{\partial \psi_\alpha}(\omega_\alpha \rho P) = \frac{\partial}{\partial \psi_\alpha} \left(\left\langle \frac{\partial}{\partial x_i} J_i^\alpha | \underline{\psi} \right\rangle \rho P \right) \\ - \frac{\partial}{\partial x_i} \left(\langle u_i'' | \underline{\psi} \rangle \rho P \right) \end{aligned} \quad (6)$$

In the above, P is the joint scalar PDF, u is the velocity, ρ is the density, ψ is the scalar space. All terms in the equation are closed except the first term on the right hand side, which is the micromixing term that needs mixing model for its closure.

4.3 Conditional Moment Closure Method

CMC model may be derived either from joint PDF method or decomposition method [45]. The major assumption made in deriving the CMC equations is that most of the fluctuations in the scalar quantities of interest could often be associated with the fluctuation of one key quantity. In non-premixed flows, where there is mixing between two bodies or streams of fluid (fuel and oxidizer), the reactive scalars within the mixing field depend strongly on the local and instantaneous value of mixture fraction $\xi(x, t)$. Conditional expectation $Q(\eta; x, t)$ of a scalar variable, conditioned on the associated value $\xi(x, t)$ taking a specific value η is defined as, $Q(\eta, x, t) = \langle \phi(x, t) | \xi(x, t) = \eta \rangle$. Here, the notation of vertical bar indicates that the average is taken of those members of the ensemble which satisfy the condition to the right of the bar. Then the local and instantaneous value of a scalar can be decomposed as,

$$\phi(x, t) = Q(\xi[x, t]; x, t) + \phi''(x, t) \quad (7)$$

The transport equation for conditional scalars may be written as,

$$\begin{aligned} \frac{\partial Q}{\partial t} + \langle u | \xi = \eta \rangle \cdot \nabla Q + \frac{1}{P(\eta)\rho_\eta} \nabla \cdot (\rho_\eta \langle u'' u'' | \xi = \eta \rangle P(\eta) \\ - \langle N | \xi = \eta \rangle \frac{\partial^2 Q}{\partial \eta^2} = \langle \dot{\omega}_F''' | \xi = \eta \rangle \end{aligned} \quad (8)$$

Here, $Q = \{Q_h, Q_\alpha\}$, and Q_h is the conditional mean enthalpy and Q_α is the conditional mean species mass fraction. In the above equation, η is the sample space variable for the mixture fraction ξ . Angular brackets denote ensemble average subject to the condition $\xi(\mathbf{x}, t) = \eta$. Also, ρ_η is the conditional density of the gaseous mixture. If closure of the conditional scalars appearing in reaction rate term which needs to be modelled is achieved at the first-moment level by neglecting the conditional fluctuations, the model is said to be ‘first-order CMC’ model. The reaction rate term in first-order CMC model with single step reaction is given by,

$$\langle \dot{\omega}_F''' | \xi = \eta \rangle = -A_F Q_F Q_O \exp\left(-\frac{E}{RQ_T}\right) \quad (9)$$

For cases where the fluctuations about conditional means of a scalar are present in significant proportions, e.g., flames with extinction and re-ignition, the closure is necessary at the second-moment level, which is known as ‘second-order CMC’ model [46]. Sometimes, another variable such as sensible enthalpy is used as the second conditioning variable [47]. CMC equations with added dimension (mixture fraction space) are solved in tandem with flow field in case of fully coupled equations. The flow solver provides the mixing field information to the CMC equations, while the CMC solver provides the information of mean density field to

the flow solver. However, CMC incurs huge computational efforts mainly due to the added dimension, namely the mixture fraction space.

5 Numerical Approaches

In this section, various modelling approaches that are used to capture autoignition are presented. In the early stage, most of the numerical work done on autoignition under turbulent conditions is based on DNS, where the problem is greatly simplified by assuming the homogeneous isotropic decaying turbulent flow like conditions.

5.1 Numerical Simulations of Autoignition in Laminar Flames

Detailed chemical mechanisms for fuel oxidation with accurate reaction rate coefficients are essential for prediction of ignition delay time using numerical simulations. Sensitivity analysis revealed that modification of reaction rate constants did not improve the prediction of ignition delay time. To improve the accuracy of the available reaction mechanism, we must include a comprehensive model that describes low-temperature reactions adequately. This allows us to predict pre-ignition heat release and ignition delay time accurately.

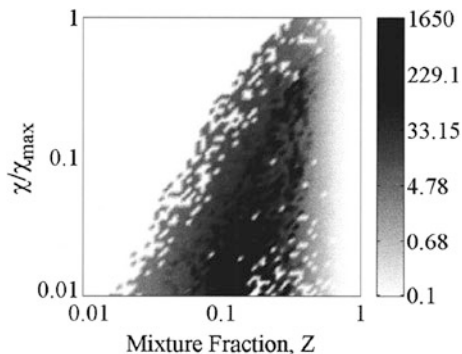
Numerical investigations were performed for autoignition in laminar flows to determine the effects of a periodic strain rate on autoignition. The results revealed that autoignition may be still likely to occur depending on the amplitude and frequency of the oscillation, even if the time-averaged scalar dissipation rate (\bar{N}) exceeds the critical scalar dissipation rate, i.e. $\bar{N} > N_{crit}$. In this case, the flow remains in a Low- N regime, which allows autoignition to take place. Converse of this situation may also happen, when $\bar{N} < N_{crit}$ moreover, the flow spends most of the time above the critical value, resulting in no autoignition.

5.2 Numerical Simulations of Autoignition in Turbulent Flames

For engineering applications, numerical approaches based on RANS and LES are being used. Due to the limitations of computational resources and the availability of reliable sub-models, the numerical modelling of autoignition under turbulent conditions has yet to achieve widespread applications.

Sreedhara and Lakshmisha [22] performed a two-dimensional DNS using a single step chemistry to study autoignition of *n*-heptane in a hot oxidizer medium.

Fig. 9 Diagram showing joint-conditional mean reaction rate during the first appearance of autoignition spots [22]

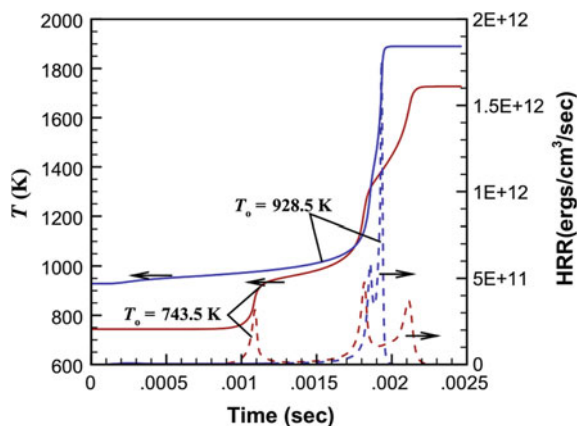


The DNS results led to a conclusion that ignition spots are favourable within some specific range of mixture fraction called the “most reactive mixture fraction” (ξ_{MR}) and also the region should have the low scalar dissipation rate, which is evident in Fig. 9 [22]. An increase in initial turbulence intensity promotes turbulent mixing and delays auto-ignition. Further, they investigated the difference between the effects of auto-ignition in two and three-dimensional flow fields using a four-step chemical kinetics. The discrepancies observed in earlier two-dimensional DNS with the experimental observations later got resolved due to the presence of vortex stretching in three-dimensional flows that are absent in two-dimensional flows [48]. Also, the first appearance of an ignition site is found to be independent of the turbulent time scale and with the increase in inhomogeneities in the mixture, the autoignition time also increases [49].

Further, they reported that the conditional scalar dissipation rate controls the ignition time and partial premixing decreases the delay in ignition time. In another DNS study [50], autoignition of DME was observed as a complex three stage process. Each stage evolves with a different chemical reaction pathway. Figure 10 shows a time history of temperature and heat release rate (HRR) for two different initial temperature conditions [50]. In the case of initial low temperature, three peaks were observed in HRR of approximately equal magnitude, and with every peak, a corresponding increase in temperature was observed. However, for the case with high initial temperature, time history of HRR showed a negligible heat release in the first stage and maximum heat release in the third stage with a comparatively very low value in the second stage.

Autoignition of hydrogen was investigated [51] in a heated co-flow using an LES—Eulerian PDF approach to model the turbulence-chemistry interaction and a detailed chemical mechanism involving 9 species and 19 reversible reactions. The model replicated the experimental results without tuning the model constants and the observed auto-ignition length matched reasonably well with the predicted auto-ignition length. The results showed a strong sensitivity to the variations in the co-flow temperature. Domingo et al. [52] investigated the lifted methane jet flames in a vitiated coflow using LES-CMC model, which established autoignition and premixed flame propagation as stabilization mechanism of flame liftoff. Further,

Fig. 10 Change in temperature and heat release rate (HRR) with time for two different initial temperatures [50]



they reported that molecular diffusion effects ignition. Recently, the effect of differential diffusion on autoignition has also been investigated [53] in a vitiated coflow with LES/PDF modelling approach. It was found that differential diffusion decreases both lift-off height and thickness of autoignition zone. Further their results showed a reasonably good prediction with experimental results and no autoignition event were observed below the liftoff height. Out of auto-ignition and turbulent flame propagation, one of the phenomenon acts as the stabilization mechanism depending upon the location across the flame length. A numerical study was carried out in [54] using analytically reduced chemistry along with the thickened flame model for turbulence-chemistry interactions. Their results showed that autoignition was the dominant flame stabilization mechanism at the flame base. Autoignition pockets were observed in the lean mixture corresponding to the “most reactive mixture fraction”. Around the centre line where the HRR is relatively high, flame propagation was found to be dominant in that region. Figure 11 shows the snapshot from the simulation, which supports the above discussion [54].

Autoignition of laminar non-premixed DME/air in a heated co-flow has been investigated [55] by varying the coflow temperature in the range of 700–1100 K. Autoignition serves as a stabilization mechanism when the coflow temperature is in the range of 700–900 K. Determination of stabilization point was carried out by the negative temperature coefficient chemistry in the mixture fraction space. At a low coflow temperature (about 700 K), the temperature was high enough to auto-ignite the gaseous mixture. However, the incoming flow velocity was not large enough to balance the flame propagation velocity. Due to this, pure kinetically stabilized flames were observed as shown in Fig. 12 [55]. On the other side, above a coflow temperature of 1100 K, the kinematic balance between the incoming flow velocity and the premixed flame propagation velocity acts as a stabilization mechanism. Figure 12 shows the change in the flame structure with respect to the change in coflow boundary temperature.

Further studies were conducted on the flame structure by varying the inlet flow velocity while keeping the coflow temperature constant [56]. When the flow

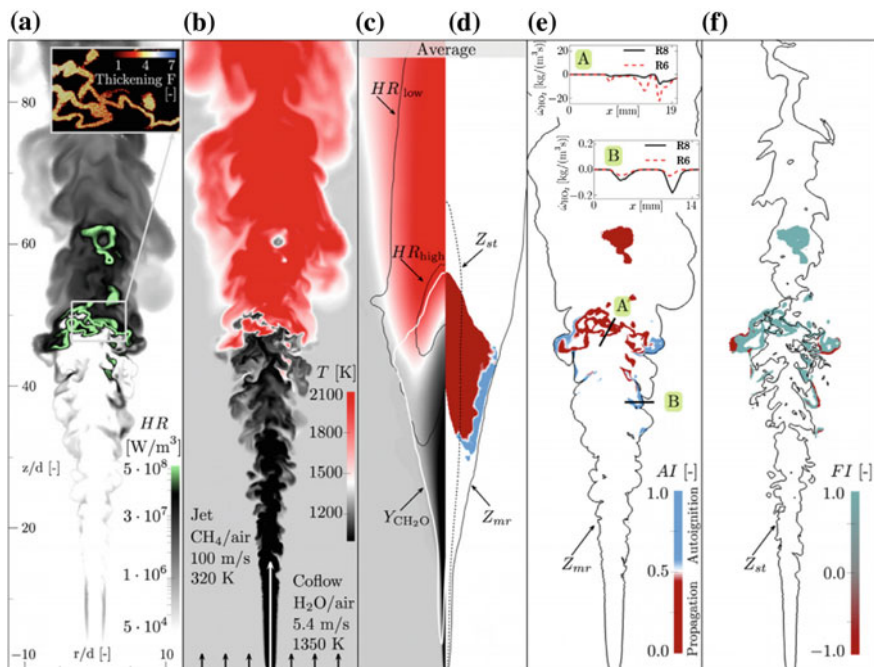


Fig. 11 Snapshots at same instant of time **a** heat release rate, **b** temperature, **c** mean temperature field, **d** The conditioned mean Autoignition field, **e** Most reactive mixture fraction superimposed on autoignition index (AI) **f** Stoichiometric mixture fraction superimposed on the flame index (FI) [54]

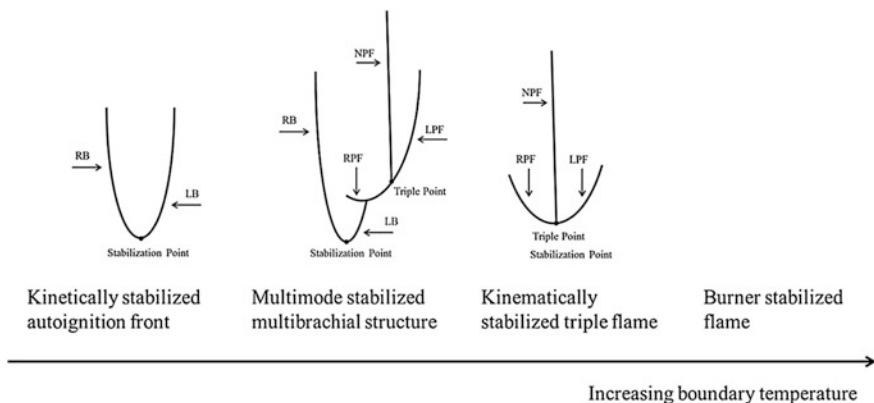
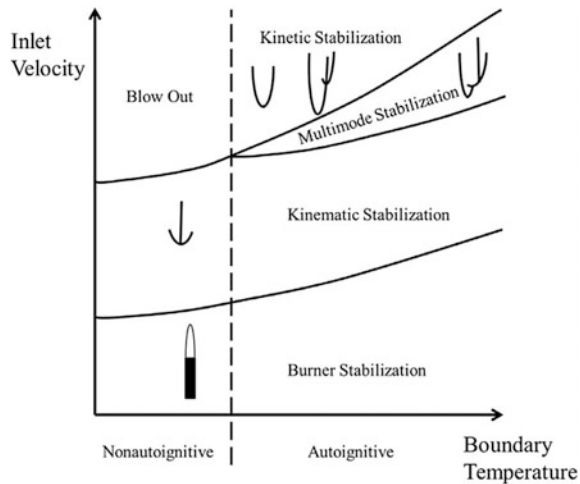


Fig. 12 Change in stabilization mechanism with a change in coflow boundary temperature [55]

velocity is 2.4 m/s, the classical triple flame structure was observed at elevated temperature due to the kinematic balance between incoming flow velocity and premixed flame propagation. With an increase in the inlet velocity, the same

Fig. 13 A regime diagram for the stabilization mechanism [56]



stabilization mechanism was not observed anymore at a certain mixture fraction values. Autoignition of inhomogeneous mixtures becomes the dominant stabilization mechanism, and a multimode stabilized flame was observed. With further increase in the inlet flow velocity, the kinematic balance was lost, and a pure kinetically balanced flame front was found. In Fig. 13, different stabilization regimes are shown as per the discussion presented here.

The applicability of the conditional moment closure (CMC) method was analysed for autoignition of *n*-heptane in a hot oxidizer medium [46]. Using DNS, a correction factor was introduced in CMC formulation for species fluctuations, which yielded the similar trend as shown by experimental results and matched well with the DNS data. The results for conditionally averaged temperature during autoignition for different eddy turnover time are shown in Fig. 14. Despite using a first order closure results were found to show an excellent agreement.

Patwardhan and Lakshmisha [57] numerically investigated auto-ignition of turbulent H_2/N_2 jets in a preheated co-flow using a RANS based first order CMC approach. They reported that modifications of $k-\epsilon$ model constants would not alter the auto-ignition length significantly shown in Fig. 15. A slight increase in autoignition length was observed due to modification of empirical constants in the turbulence model, which resulted in reduced variance and increased mixing. This suggests autoignition process is primarily controlled by chemical kinetics rather than mixing. They concluded that first order CMC was unable to produce random spots that were observed in experimental results. The time sequences of autoignition and subsequent flame development are shown in Fig. 16 for different coflow temperature. Flashback is observed at all coflow temperature and random spots are not found due to the incapability of RANS because it averaged out the scalar field and unable to reproduce it.

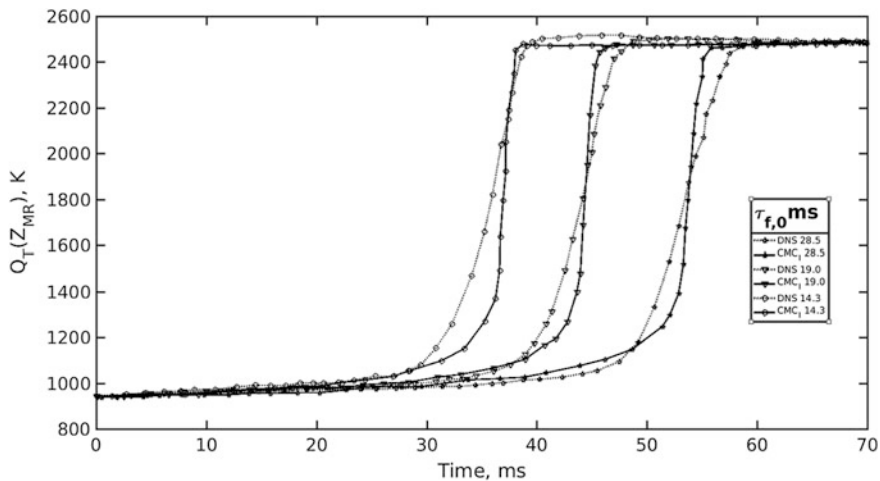


Fig. 14 Time history of conditionally averaged temperature $Q_T(Z_{MR})$ during autoignition comparison against DNS data for different initial eddy-turnover times [46]

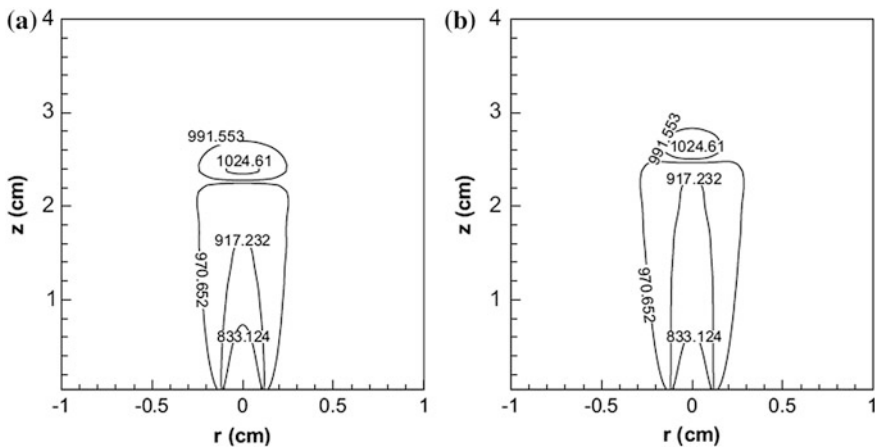


Fig. 15 Contours of mean temperature at the time of autoignition: **a** standard $k-\epsilon$ at $t = 0.938$ ms, and **b** modified $k-\epsilon$ at $t = 1.019$ ms [57]

The effects of fluctuations of conditional scalar dissipation rate have also been included in the numerical model of [49] and found the autoignition time, and that shows a reasonably good agreement with DNS results. Wu et al. [58] investigated numerically ethanol and DME lifted flames in a hot vitiated co-flow. They used an eddy dissipation concept (EDC) model in the RANS context for turbulence-chemistry interaction. They concluded that value of the mixture fraction for the two

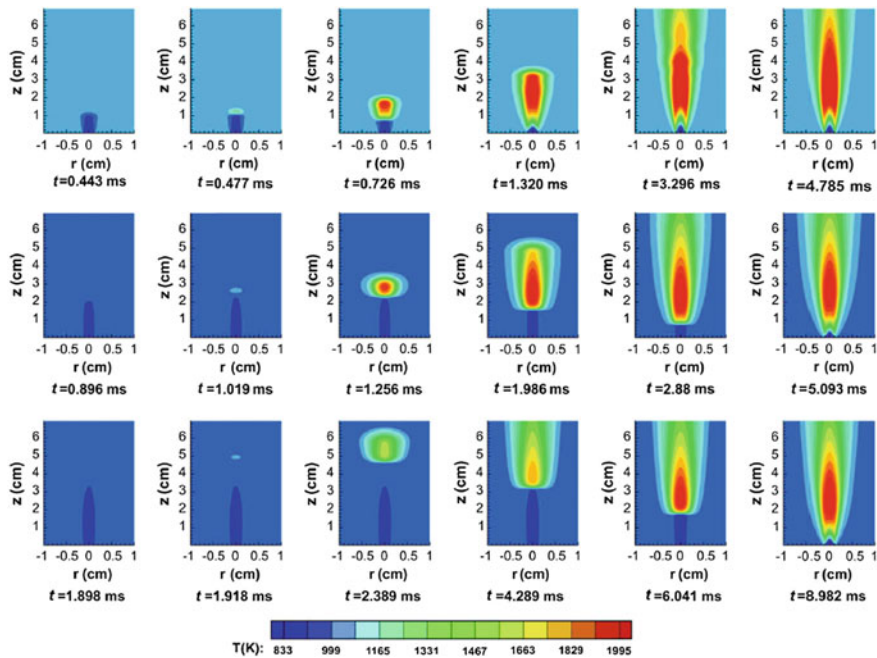


Fig. 16 Contours of mean temperature at different time instances for different coflow temperature: $T_{\text{coflow}} = 1020$ K (top row), $T_{\text{coflow}} = 980$ K (middle row), and $T_{\text{coflow}} = 960$ K (bottom row) [57]

fuels is same at the stabilization point under identical conditions. Also, before auto-ignition, stabilization point was found to be affected simultaneously by ignition delay and reaction paths of the fuel under low co-flow temperature. However, at high co-flow temperature, lift off height is mainly controlled by ignition delay. Further, at high co-flow temperature flame stabilizes in the leaner mixture. The first-order spatially averaged CMC model was used to study auto-ignition of a gaseous *n*-heptane plume in a heated co-flow [3]. They concluded that the conditional scalar dissipation rate is much smaller value than the critical value for a perceptible span before auto-ignition takes place. After the critical value of conditional scalar dissipation rate, auto-ignition was observed.

Effect of DME dilution in natural gas was examined numerically in an HCCI engine [59] with detailed chemical kinetics to describe the low-temperature autoignition chemistry. The CHEMKIN chemistry solver was integrated with KIVA-3V CFD code for solving the multidimensional engine simulations. The numerical model used in [59] gave a reasonably good level of agreement with the available experimental results. A two-step ignition process was observed, where initially DME controls the ignition by self-oxidation before the major oxidation of natural gas could take place. With an increase in DME concentration in the natural gas, the ignition delay time decreases due to auto-ignition of DME at a relatively

low temperature than methane. With an increase in natural gas concentration, the engine becomes unstable because operating range becomes narrower for very low excess air-fuel ratio of natural gas.

6 Conclusions

This chapter seeks to provide an overview on autoignition in laminar and turbulent nonpremixed flames. Various burners used for experimental investigations are reviewed along with the available numerical approaches with a specific attention for autoignition under turbulent conditions. Although substantial progress has been made in this area, we are yet to address several unresolved issues. The major findings and future research directions are summarized below:

- Autoignition of the fuel occurs at the specific temperature depending upon its physical and chemical properties for the given value of the strain rate. For a specific temperature, autoignition does not occur above a critical value of strain rate. Further, autoignition temperature increases with an increase in strain rate.
- The autoignition in non-premixed systems occurs at some specific value of mixture fraction usually away from the stoichiometric value of mixture fraction, referred as “most reactive mixture fraction”. Autoignition is also found to be a dominant stabilization mechanism at the flame base of a lifted flame.
- Experimental data on autoignition in turbulent non-premixed flames are limited and only available for very simple flow configurations. Most of the work done on turbulent autoignition is specifically focused on the Berkley vitiated coflow burner and Cambridge confined turbulent hot coflow burner. More detailed experiments should be planned to investigate the direct effect of turbulence on autoignition in enclosed flow geometry.
- More experiments should be directed to investigate autoignition and subsequent flame development at the high-pressure environment using the heated oxidizer/product stream. Further, autoignition characteristics of synthetic fuels, alcohols, and different fuel mixtures under turbulent conditions should be investigated, before introducing them into the practical energy conversion systems.
- On the modelling side, new combustion models are needed to develop which consider the nature of flame propagation in mixtures with large mixture fraction fluctuations. Applications of higher order conditioning methods may be useful for the flames undergoing large mixture fraction fluctuations.
- New reaction mechanisms are needed to be developed, which are valid in a wide range of temperature and pressure. Moreover, suitably reduced chemical mechanisms for different fuel and fuel mixtures needs to be explored for their applications in numerical codes using advanced turbulent combustion models, namely, transported or stochastic PDF approach, and CMC method.

References

1. Cabra R, Myhrvold T, Chen JY, Dibble RW, Karpetis AN, Barlow RS (2002) Simultaneous laser Raman-Rayleigh-Lif measurements and numerical modeling results of a lifted turbulent H-2/N-2 jet flame in a vitiated coflow. *Proc Combust Inst* 29:1881–1888
2. Markides CN, Mastorakos E (2005) An experimental study of hydrogen autoignition in a turbulent co-flow of heated air. *Proc Combust Inst* 30:883–891
3. Markides CN, De Paola G, Mastorakos E (2007) Measurements and simulations of mixing and autoignition of an n-heptane plume in a turbulent flow of heated air. *Exp Therm Fluid Sci* 31:393–401
4. Gordon RL, Masri AR, Mastorakos E (2008) Simultaneous Rayleigh temperature, OH- and CH2O-LIF imaging of methane jets in a vitiated coflow. *Combust Flame* 155:181–195
5. Gordon RL, Masri AR, Mastorakos E (2009) Heat release rate as represented by $[OH] \times [CH_2O]$ and its role in autoignition. *Combust Theory Model* 13:645–670
6. Park SH, Lee CS (2014) Applicability of dimethyl ether (DME) in a compression ignition engine as an alternative fuel. *Energy Convers Manag* 86:848–863
7. Das LM (1990) Fuel induction techniques for a hydrogen operated engine. *Int J Hydrog Energy* 15:833–842
8. Semelsberger TA, Borup RL, Greene HL (2006) Dimethyl ether (DME) as an alternative fuel. *J Power Sources* 156:497–511
9. Carlier M, Corre C, Minetti R, Pauwels JF, Ribaucour M, Sochet LR (1991) Autoignition of butane: a burner and a rapid compression machine study. *Symp (Int) Combust* 23:1753–1758
10. Shi Z, Zhang H, Liu H, Lu H, Li J, Gao X (2015) Effects of buffer gas composition on autoignition of dimethyl ether. *Energies* 8:10198
11. Pitz WJ, Wilk RD, Westbrook CK, Cernansky NP (1988) Western States Section of the Combustion Institute
12. Minetti R, Ribaucour M, Carlier M, Fittschen C, Sochet LR (1994) Experimental and modeling study of oxidation and autoignition of butane at high-pressure. *Combust Flame* 96:201–211
13. Kukkadapu G, Weber BW, Sung CJ (2015) Autoignition study of tetralin in a rapid compression machine at elevated pressures and low-to-intermediate temperatures. *Fuel* 159:436–445
14. Yetter RA, Dryer FL, Rabitz H (1991) Flow reactor studies of carbon-monoxide hydrogen oxygen kinetics. *Combust Sci Technol* 79:129–140
15. Schonborn A, Sayad P, Konnov AA, Klingmann J (2014) OH*-chemiluminescence during autoignition of hydrogen with air in a pressurised turbulent flow reactor. *Int J Hydrog Energy* 39:12166–12181
16. Schonborn A, Sayad P, Konnov AA, Klingmann J (2014) Autoignition of dimethyl ether and air in an optical flow-reactor. *Energy Fuel* 28:4130–4138
17. Schonborn A, Sayad P, Konnov AA, Klingmann J (2013) Visualisation of propane autoignition in a turbulent flow reactor using OH* chemiluminescence imaging. *Combust Flame* 160:1033–1043
18. Beerer DJ, McDonnell VG (2008) Autoignition of hydrogen and air inside a continuous flow reactor with application to lean premixed combustion. *J Eng Gas Turb Power* 130
19. Oehlschlaeger MA, Steinberg J, Westbrook CK, Pitz WJ (2009) The autoignition of iso-cetane at high to moderate temperatures and elevated pressures: shock tube experiments and kinetic modeling. *Combust Flame* 156:2165–2172
20. Wang WJ, Oehlschlaeger MA (2012) A shock tube study of methyl decanoate autoignition at elevated pressures. *Combust Flame* 159:476–481
21. Mastorakos E (2009) Ignition of turbulent non-premixed flames. *Prog Energy Combust* 35:57–97
22. Sreedhara S, Lakshmisha KN (2000) Direct numerical simulation of autoignition in a non-premixed, turbulent medium. *Proc Combust Inst* 28:25–33

23. Fotache CG, Kreutz TG, Zhu DL, Law CK (1995) An experimental study of ignition in nonpremixed counterflowing hydrogen versus heated air. *Combust Sci Technol* 109:373–393
24. Fotache CG, Kreutz TG, Law CK (1997) Ignition of hydrogen-enriched methane by heated air. *Combust Flame* 110:429–440
25. Zheng XL, Lu TF, Law CK, Westbrook CK, Curran HJ (2005) Experimental and computational study of nonpremixed ignition of dimethyl ether in counterflow. *Proc Combust Inst* 30:1101–1109
26. Sepman A, Abtahizadeh E, Mokhov A, van Oijen J, Levinsky H, de Goey P (2013) Experimental and numerical studies of the effects of hydrogen addition on the structure of a laminar methane-nitrogen jet in hot coflow under MILD conditions. *Int J Hydrog Energy* 38:13802–13811
27. Sepman AV, Abtahizadeh SE, Mokhov AV, van Oijen JA, Levinsky HB, de Goey LPH (2013) Numerical and experimental studies of the NO formation in laminar coflow diffusion flames on their transition to MILD combustion regime. *Combust Flame* 160:1364–1372
28. Cabra R, Chen JY, Dibble RW, Karpetis AN, Barlow RS (2005) Lifted methane-air jet flames in a vitiated coflow. *Combust Flame* 143:491–506
29. Markides CN, Mastorakos E (2011) Experimental investigation of the effects of turbulence and mixing on autoignition chemistry. *Flow Turbul Combust* 86:585–608
30. Roubaud A, Lemaire O, Minetti R, Sochet LR (2000) High pressure auto-ignition and oxidation mechanisms of o-xylene, o-ethyltoluene, and n-butylbenzene between 600 and 900 K. *Combust Flame* 123:561–571
31. Johannessen B, North A, Dibble R, Lovas T (2015) Experimental studies of autoignition events in unsteady hydrogen-air flames. *Combust Flame* 162:3210–3219
32. Papageorge MJ, Arndt C, Fuest F, Meier W, Sutton JA (2014) High-speed mixture fraction and temperature imaging of pulsed, turbulent fuel jets auto-igniting in high-temperature, vitiated co-flows, *Exp Fluids* 55
33. Fast G, Kuhn D, Class AG, Maas U (2009) Auto-ignition during instationary jet evolution of dimethyl ether (DME) in a high-pressure atmosphere. *Combust Flame* 156:200–213
34. Oldenhof E, Tummers MJ, van Veen EH, Roekaerts DJEM (2012) Transient response of the Delft jet-in-hot coflow flames. *Combust Flame* 159:697–706
35. Z. Chen, M. Konno, M. Oguma, T. Yanai, Experimental Study of CI Natural-Gas/DME Homogeneous Charge Engine, SAE International, 2000
36. Venkatesan M, Moorthi NSV, Karthikeyan R, Manivannan A (2014) Experimental study on hydrous methanol fuelled hcci engine using air pre-heater assisted controlled autoignition. *Trans Famena* 38:53–66
37. Maurya RK, Agarwal AK (2014) Experimental investigations of performance, combustion and emission characteristics of ethanol and methanol fueled HCCI engine. *Fuel Process Technol* 126:30–48
38. Pope SB (1985) Pdf methods for turbulent reactive flows. *Prog Energy Combust* 11:119–192
39. Peters N (1984) Laminar diffusion flamelet models in non-premixed turbulent combustion. *Prog Energy Combust* 10:319–339
40. Veynante D, Vervisch L (2002) Turbulent combustion modeling. *Prog Energy Combust* 28:193–266
41. Peters N (1999) The turbulent burning velocity for large-scale and small-scale turbulence. *J Fluid Mech* 384:107–132
42. Subramaniam S, Pope SB (1998) A mixing model for turbulent reactive flows based on Euclidean minimum spanning trees. *Combust Flame* 115:487–514
43. Subramaniam S, Pope SB (1999) Comparison of mixing model performance for nonpremixed turbulent reactive flow. *Combust Flame* 117:732–754
44. Bilger RW (2000) Future progress in turbulent combustion research. *Prog Energy Combust* 26:367–380
45. Klimenko AY, Bilger RW (1999) Conditional moment closure for turbulent combustion. *Prog Energy Combust* 25:595–687

46. Sreedhara S, Lakshmisha KN (2002) Assessment of conditional moment closure models of turbulent autoignition using DNS data. *Proc Combust Inst* 29:2069–2077
47. Kronenburg A (2004) Double conditioning of reactive scalar transport equations in turbulent nonpremixed flames. *Phys Fluids* 16:2640–2648
48. Sreedhara S, Lakshmisha KN (2002) Autoignition in a non-premixed medium: DNS studies on the effects of three-dimensional turbulence. *Proc Combust Inst* 29:2051–2059
49. Mastorakos E, Baritaud TA, Poinot TJ (1997) Numerical simulations of autoignition in turbulent mixing flows. *Combust Flame* 109:198–223
50. Bansal G, Mascarenhas A, Chen JH (2015) Direct numerical simulations of autoignition in stratified dimethyl-ether (DME)/air turbulent mixtures. *Combust Flame* 162:688–702
51. Jones WP, Navarro-Martinez S (2007) Large eddy simulation of autoignition with a subgrid probability density function method. *Combust Flame* 150:170–187
52. Domingo P, Vervisch L, Veynante D (2008) Large-eddy simulation of a lifted methane jet flame in a vitiated coflow. *Combust Flame* 152:415–432
53. Han W, Raman V, Chen Z (2016) LES/PDF modeling of autoignition in a lifted turbulent flame: analysis of flame sensitivity to differential diffusion and scalar mixing time-scale. *Combust Flame* 171:69–86
54. Schulz O, Jaravel T, Poinot T, Cuenot B, Noiray N (2016) A criterion to distinguish autoignition and propagation applied to a lifted methane–air jet flame, *P Combust Inst*, doi:[10.1016/j.proci.2016.08.022](https://doi.org/10.1016/j.proci.2016.08.022)
55. Deng SL, Zhao P, Mueller ME, Law CK (2015) Autoignition-affected stabilization of laminar nonpremixed DME/air coflow flames. *Combust Flame* 162:3437–3445
56. Deng SL, Zhao P, Mueller ME, Law CK (2015) Stabilization of laminar nonpremixed DME/air coflow flames at elevated temperatures and pressures. *Combust Flame* 162:4471–4478
57. Patwardhan SS, Lakshmisha KN (2008) Autoignition of turbulent hydrogen jet in a coflow of heated air. *Int J Hydrog Energy* 33:7265–7273
58. Wu ZJ, Zhang Q, Bao TT, Li LG, Deng J, Hu ZJ (2016) Experimental and numerical study on ethanol and dimethyl ether lifted flames in a hot vitiated co-flow. *Fuel* 184:620–628
59. Kong SC (2007) A study of natural gas/DME combustion in HCCI engines using CFD with detailed chemical kinetics. *Fuel* 86:1483–1489

Combustion for Power Generation and Transportation
Technology, Challenges and Prospects

Agarwal, A.K.; De, S.; Pandey, A.; Singh, A.P. (Eds.)

2017, X, 451 p. 240 illus., 178 illus. in color., Hardcover

ISBN: 978-981-10-3784-9